# Two-Dimensional Solid-State $^1$H-NMR and Proton Exchange†

**Ling Zheng,‡,§ Kenneth W. Fishbein,§,∥ Robert G. Griffin,§,∥ and Judith Herzfeld*,‡**

*Contribution from the Department of Chemistry, Brandeis University, Waltham, Massachusetts 02254-9110, and the Francis Bitter National Magnet Laboratory and Department of Chemistry, Massachusetts Institute of Technology, Cambridge, Massachusetts 02139-4307*

*Received January 28, 1993*

**Abstract:** High-resolution solid-state $^1$H NMR spectra were obtained by combining deuterium spin-dilution and high-speed magic-angle spinning (MAS). The effective proton relaxation time $T_1$, which is long in these magnetically dilute samples, was reduced by reverse cross-polarization (RCP) of protons from deuterons. Two-dimensional $^1$H NOESY spectra obtained with RCP were used to investigate proton exchange in solids, and the rapid proton exchange observed in this way was linked to hydrogen bonds. A quantitative analysis of the dependence of the 2D spectral intensities on mixing time, as a function of temperature, was employed to determine the rates, and activation energies, for proton/deuteron exchange between the carboxyl groups of the oxalate moiety and the water of hydration in oxalic acid dihydrate. We find rate constants of 55 and 58 $s^{-1}$ at 17 °C and activation energies of 8.5 and 8.9 kcal/mol over the temperature range −26 to 28 °C.

## Introduction

Solution proton NMR has become an increasingly powerful structural tool in chemistry and biophysics. In contrast, the resolution in solid-state proton NMR at currently accessible field strengths (300–600 MHz) is normally limited by strong proton dipolar interactions, which are incompletely attenuated.[1] Magic angle spinning (MAS) was first introduced in solid-state NMR to average these homonuclear dipolar interactions by mechanical rotation of the sample. However, since the proton dipolar interaction is typically much larger than the sample spinning speed (~40–50 kHz vs <23 kHz), MAS alone is insufficient to obtain high-resolution $^1$H spectra in solids. Multiple pulse techniques, such as WAHUHA, MREV-8, and BR-24, etc., were also developed to attenuate proton dipolar interactions, and ideally, these techniques can suppress homonuclear dipolar interactions, leaving the chemical shift anisotropy (CSA) as the only significant term in the Hamiltonian. Since the CSA for protons is small enough to be averaged by MAS, the combination of multiple pulse techniques with MAS, known as CRAMPS (combined rotation and multiple pulse spectroscopy),[2] in principle, can reduce the proton line widths in a spectrum of an ordinary organic solid to a few hundred hertz. However, as a practical matter, such results are difficult to achieve.

Proton dipolar interactions can also be reduced by chemically exchanging protons with deuterons, thereby increasing the average proton internuclear distance.[3] Work from this laboratory has recently demonstrated that better resolution can be obtained in the $^1$H spectra of alanine by random spin-dilution than by multiple pulse methods.[4]

Here, we demonstrate that the method of spin-dilution can be applied to compounds for which deuterium exchange of all sites can be achieved to a level of about 90%. As expected, since magnetic dilution breaks the proton relaxation pathway, the proton spin–lattice relaxation time $T_1$ increases dramatically upon deuteration. However, we also show that by applying reverse cross-polarization (RCP) from deuterons to protons, to take advantage of the relatively short $T_1$ of deuterium, well-resolved 1D and 2D $^1$H spectra can be obtained in a reasonable amount of time. This method is used to obtain proton 2D-RCP spectra of chemically exchanging systems, where the exchange is mediated by hydrogen bonds. The proton exchange rates are obtained directly from the spectra, and the temperature dependence of these exchange rates yields the Arrhenius activation energy for proton exchange.

## Methods

**Sample Preparation.** Deuterated oxalic acid dihydrate ($HOX\cdot 2H_2O$) was prepared by dissolving 10.1 g of oxalic acid dihydrate crystal ($H_2C_2O_4\cdot 2H_2O$, Mallinckrodt, AR) in 45 mL of deuterium oxide ($D_2O$, Cambridge Isotope Laboratories, D 99.9 atom %), yielding a proton-to-deuteron ratio of 1:9. Crystals of deuterated $\alpha$-oxalic acid dihydrate[5] were grown at room temperature for 3 days, ground to a powder, and packed into an NMR rotor. The sample was analyzed for water content using Karl Fisher titration (Mettler DL18).

The 90% deuterated ammonium hydrogen oxalate hemihydrate ($AHOX\cdot {}^1/_2H_2O$) sample was prepared by crystallization from a stoichiometric mixture of 4.7 g of oxalic acid dihydrate (Mallinckrodt) and 5.4 g of ammonium oxalate monohydrate (Fisher Scientific Co.) in 56 mL of $D_2O$.[6]

The sample of 90% deuterated $(AHOX:HOX)\cdot 2H_2O$ was prepared by stoichiometrically dissolving 64.8 g of oxalic acid dihydrate (Mallinckrodt) in 20 mL of $NH_4OH$ (Mallinckrodt, AR 58%) with 110 mL of $H_2O$ and recrystallizing. Next 9.3-g of these crystals were dissolved in 45 mL of $D_2O$ for deuterium exchange and the deuterated $(AHOX:HOX)\cdot 2H_2O$ was then recrystallized. The chemical analysis of this material gave a stoichiometry of $NH_{11}C_4O_{10}$ (Galbraith Laboratories, Knoxville, TN). X-ray crystallographic studies verified the chemical analysis and found a crystal structure of space group $P\bar{1}$ with two ammonium hydrogen oxalate molecules, two oxalic acid molecules, and four water molecules in a unit cell with $a = 6.343$ Å, $b = 7.231$ Å, $c = 10.575$ Å, $\alpha = 85.68°$, $\beta = 79.61°$, and $\gamma = 97.83°$.[7]

Crystals of alanine approximately 98% deuterated at the $\alpha$-carbon and approximately 99% deuterated at the methyl group were prepared

† L.Z. wishes to dedicate his contribution to this work to his late sisters, Juan Zheng (*1955–1991*) and Wei Zheng (*1962–1991*), for their loving memories and encouragement.

‡ Department of Chemistry, Brandeis University.

§ Francis Bitter National Magnet Laboratory, MIT.

∥ Department of Chemistry, MIT.

(1) Sekine, S.; Kubo, A.; Sano, H. *Chem. Phys. Lett.* **1990**, *171*, 155–160.
(2) Maciel, G. E.; Bronnimann, C. E.; Hawkins, B. L. *Adv. Magn. Reson.* **1990**, *14*, 125–150.
(3) Eckman, R. *J. Chem. Phys.* **1982**, *76*, 2767–2768.
(4) McDermott, A. E.; Creuzet, F. J.; Kolbert, A. C.; Griffin, R. G. *J. Magn. Reson.* **1992**, *98*, 408–413.
(5) Iwasak, F. F.; Saito, Y. *Acta Crystallogr.* **1967**, *23*, 56–63. Iwasak, F. F.; Iwasak, H.; Saito, Y. *Acta Crystallogr.* **1967**, *23*, 64–70.
(6) Fernandes, N. G.; Tellgren, R. *Acta Crystallogr.* **1989**, *C45*, 499–504.
(7) Foxman, B.; Zheng, L. In preparation.

0002-7863/93/1515-6254$04.00/0 

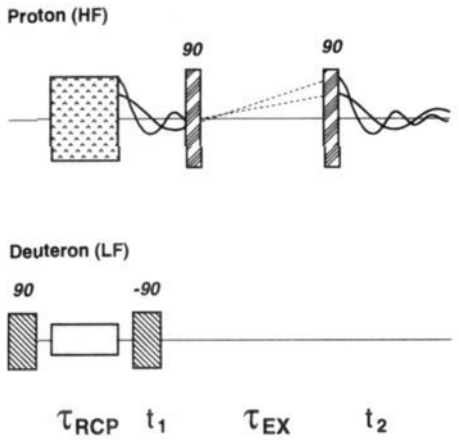


**Figure 1.** Pulse sequence used for acquiring two-dimensional $^1$H spectra with deuterium-to-proton cross-polarization and deuterium flip-back (–90°) pulse.

by dissolving and re-crystallizing 222 mg of L-alanine-$d_4$ (MSD, D 98.8 atom %) with 3 mg of L-alanine-3,3,3-$d_3$ (MSD, D 99.4 atom %) in 2 mL of deuterium oxide. The alanine was recrystallized 5 times from 3 mL of $D_2O$ to increase the deuteration of the amino group. Similar procedures were followed for preparing other amino acids.

Crystals of lithium hydrazinium sulfate were prepared by recrystallizing stoichiometric amounts of $Li_2CO_3$ (Fluka-Garantie) and $H_2NNH_2{\cdot}H_2SO_4$ (Aldrich) in $D_2O$, according to Brown and Frech.[8]

**Spectroscopy.** NMR spectra were recorded at room temperature, except where otherwise stated, on a home-built spectrometer operating at a proton frequency of 397.7 MHz. The home-built double-resonance solid-state NMR probe was equipped with a 5-mm high-speed rotor assembly (Doty Scientific Inc.) and had a $^1$H 90° pulse of 3.5 μs. The sample spinning speed was ~10 kHz. One-dimensional spectra were collected with echo detection. The magic angle was adjusted by observing the $^2$H rotational echo spectrum. The pulse sequence used to acquire two-dimensional chemical exchange spectra with reverse cross-polarization is shown in Figure 1. Typically the deuterium 90° pulse was 4.6 μs and the RCP time ($\tau_{RCP}$) varied from 0.1 to 1.0 ms. Since the deuterium $T_1$ can become very long at low temperatures (e.g. 0.9 and 3.6 s for $HOX{\cdot}2H_2O$ at –22 and –49 °C, respectively), a second "flip-back pulse" was added to the sequence to reduce the experimental recycle delay. A typical 2D-RCP spectrum with 128 $t_1$ spectra was collected in approximately 2–3 h depending on the length of the mixing time. The free induction decays in $t_1$ of 2D spectra were extended by linear prediction algorithms to 512 points and then zero-filled to 1024 points.

## Results

**$^1$H Solid-State Spectra.** Figure 2 shows $^1$H MAS spectra obtained for several deuterated, solid samples.

Alanine is used in our experiments as a resolution standard, because the width of the alanine methyl group (D 99 atom %) resonance is the narrowest $^1$H line observed thus far (full-width at half-height of 0.18 ppm). The narrow line width is due in part to rapid motion of the methyl group and the high deuterium content of this sample. The downfield shoulder on the $-NH_3^+$ resonance at 8.41 ppm is thought to be due to the $^{14}$N nucleus. Similar but smaller effects are also observed in the proton spectra of aspartic acid and serine, as shown in Figure 2. The data for alanine in Table I indicate that the line widths depend only weakly on spinning speed, i.e. when the spinning speed was increased from 4.2 to 11.2 kHz, the line widths decreased by 27% for the methyl group, 14% for the α proton, and 5% for the amino group. On the other hand, the side-band intensities are dramatically affected by the spinning speed. At 11.2 kHz, the side-band intensities dropped to 33% ($NH_3^+$), 30% (CH), and 24% ($CH_3$) of their values at 4.2 kHz or 6% ($NH_3^+$), 6% (CH), and 3% ($CH_3$) of their values at 3.1 kHz. At less than 5% of the center-band intensities, the side-band intensities can be neglected in numerical analyses. Therefore, although a high spinning speed is not crucial from the point of view of line width, it is important to eliminate the complications of side-band intensities. For this reason, all of the results reported here are for spinning speeds at or above 9.5 kHz (malonic acid was the only exception, which was measured at 8.5 kHz).

A noteworthy feature of the alanine spectrum is that the relative intensities do not have a one-to-one relationship to their chemical compositions but rather reveal the degree of protonation/deuteration. Thus, in this particular alanine sample, the methyl group is protonated at a lower level than the amino protons. This feature is also apparent in the other spectra in Figure 2.

Since we are interested in proton exchange in solids, all the other samples in Figure 2 have the common feature that they

(8) Brown, S. H.; Frech, R. *Solid State Ionics* **1986**, *18* & *19*, 1020–1024.

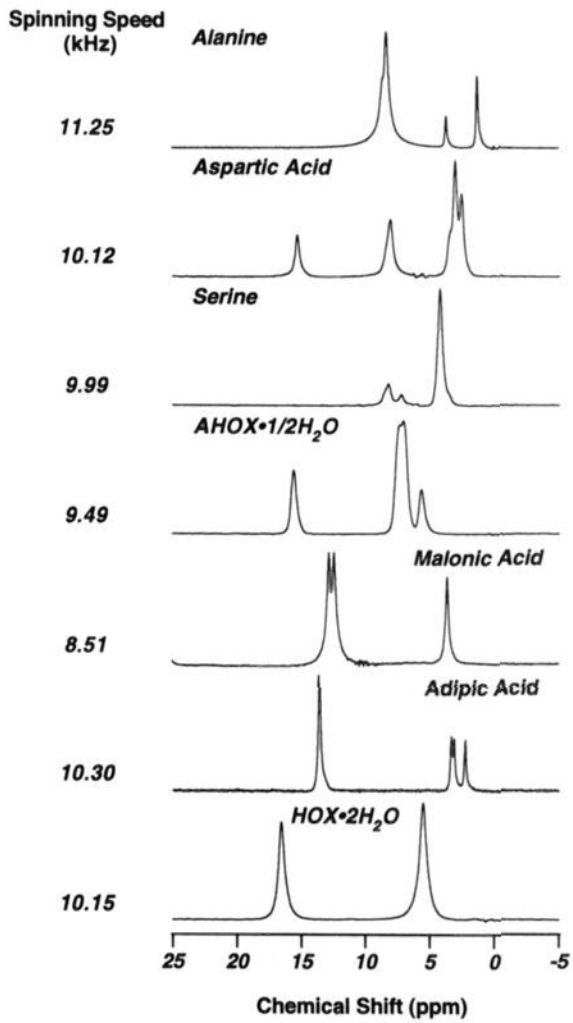


**Figure 2.** Bloch decay $^1$H-SSNMR spectra of isotopically diluted solids at room temperature.

**Table I.** $^1$H Side-Band Intensities and Full-Widths at Half-Height of Deuterated Alanine at Different Magic Angle Spinning Speeds

| spinning speed (kHz) | av of intensities of first side bands (% of center bands) | | | full-widths at half-height (ppm) | | |
|---|---|---|---|---|---|---|
| | $NH_3^+$ | CH | $CH_3$ | $NH_3^+$ | CH | $CH_3$ |
| 3.1[a] | 26.1 | 19.1 | 18.8 | 0.73 | 0.27 | 0.44 |
| 4.2 | 15.8 | 12.3 | 10.2 | 0.69 | 0.23 | 0.25 |
| 5.5 | 11.1 | 9.4 | 6.5 | 0.67 | 0.23 | 0.23 |
| 7.5 | 7.8 | 6.2 | 4.2 | 0.65 | 0.22 | 0.20 |
| 9.5 | 6.2 | 4.9 | 2.9 | 0.64 | 0.21 | 0.19 |
| 11.2 | 5.2 | 3.6 | 2.5 | 0.65 | 0.20 | 0.19 |

[a] Due to the partial overlap of side-bands at this spinning speed, the measurement of side-band intensities and full-widths at half-height could not be as accurate as at other speeds.

Table II. $^1H$ Chemical Shifts (ppm, TMS)

| | COOH | $NH_3^+$ | $NH_4^+$ | OH | $H_2O$ | CH | $CH_2$ | $CH_3$ |
|---|---|---|---|---|---|---|---|---|
| alanine | | 8.41 | | | | 3.74 | | 1.32 |
| aspartic acid | 15.36 | 8.12 | | | | 3.10 | 2.59 | |
| serine | | 8.26 | | 7.24 | | 4.25 | 3.48 | |
| AHOX | 15.61 | | 7.37 | | 5.68 | | | |
| | | | 7.07 | | | | | |
| malonic acid | 12.86 | | | | | | 3.67 | |
| | 12.48 | | | | | | | |
| adipic acid | 13.63 | | | | | | 3.36 | |
| | | | | | | | 3.15 | |
| | | | | | | | 2.27 | |
| HOX | 16.56 | | | | 5.53 | | | |
| AHOX:HOX | 18.02 | | 6.54 | | 5.71 | | | |
| | 17.54 | | | | 6.54 | | | |
| | 15.52 | | | | | | | |

Table III. $^1H$ Full-Widths at Half-Height of Oxalic Acid Dihydrate Uniformly Deuterated at Different Levels Measured at 397.7 MHz

| | full-widths at half-height (Hz) | |
|---|---|---|
| protonation $(H/(H+D)$ %) | COOH | $H_2O$ |
| 2.5 | 150 | 170 |
| 5.0 | 200 | 240 |
| 10.0 | 250 | 310 |
| 25.0 | 510 | 670 |
| 50.0 | 790 | 1020 |

possess potentially exchangeable protons. These protons are normally exchangeable with deuterons and therefore are not observable in solution proton NMR experiments. The chemical shifts for all the compounds in Figure 2 are listed in Table II. Some of these chemical shifts have been measured in multiple-pulse and/or single-crystal experiments.[9,10] In the case of malonic acid, BR-24 CRAMPS results gave carboxyl proton shifts at 12.78 and 12.42 ppm and a $CH_2$ shift at 3.50 ppm,[10] thus the splitting of carboxyl resonance, due to hydrogen bonding, was 0.36 ppm and the average carboxyl shift (12.60 ppm) was 9.10 ppm downfield from the $CH_2$ resonance. This is very similar to our carboxyl splitting of 0.38 ppm and our 9.00 ppm downfield shift of the average carboxyl resonance relative to $CH_2$. Thus, as expected, deuteration has not changed the electronic structures significantly.

As indicated above the proton/deuterium ratio is expected to affect the spectral line widths. This effect is illustrated in Table III for uniformly deuterated oxalic acid dihydrate at three different levels of protonation up to 50%. Here the line width is seen to increase less than linearly with protonation at high spinning speeds. The $^1H$–$^2H$ dipolar interaction is inhomogeneous in the sense of Maricq and Waugh[11] and is removed by MAS. Thus, $^2H$ decoupling did not improve the resolution of the $^1H$ spectra. The need for high-speed MAS arises from residual $^1H$ homonuclear dipolar interactions.

**Reverse Cross-Polarization (RCP).** The proton dipolar interaction depends on the distance $r_{12}$ between two protons according to the Hamiltonian[12]

$$H^0_{1,2} = (\gamma^2\hbar/r_{12}^3)\{I_1\cdot I_2 - 3I_{z1}I_{z2}\} \quad (1)$$

where $\gamma$ is the proton gyromagnetic ratio; $\hbar$ is Planck's constant divided by $2\pi$; $I_1$ and $I_2$ are the spin operators of protons 1 and 2, with $z$ components (along the field $B_0$) $I_{z1}$ and $I_{z2}$. Since the proton spin–lattice relaxation rate varies in proportion to $r_{12}^6$,[12]

(9) Scheler, G.; Haubenreisser, U.; Rosenberger, H. *J. Magn. Reson.* **1981**, *44*, 134–144. Berglund, B.; Vaugham, R. W. *J. Chem. Phys.* **1980**, *73*, 2037–2043. Jeffrey, G. A.; Yeon, Y. *Acta Crystallogr.* **1986**, *B42*, 410–413. Kaliaperumal, R.; Sears, R. E. J.; Ni, Q. W.; Furst, J. E. *J. Chem. Phys.* **1989**, *91*, 7387–7391.

(10) Burum, D. P. *Concepts Magn. Reson.* **1990**, *2*, 213–227.

(11) Maricq, M. M.; Waugh, J. S. *J. Chem. Phys.* **1979**, *70*, 3300–3316.

(12) Goldman, M. *Quantum Description of High-Resolution NMR in Liquids*; Clarendon Press: Oxford, 1988; pp 243–248.

Table IV. $^1H$ Spin-Lattice Relaxation Times $T_1$ and $^1H$ Spin–Spin Relaxation Times $T_2$ for Deuterated Oxalic Acid Dihydrate

| | $T_1$(s)[a] | | $T_2$ (ms)[b] | |
|---|---|---|---|---|
| protonation $[H/(H+D)$ %] | COOH | $H_2O$ | COOH | $H_2O$ |
| 2.5 | 120 | 130 | 3.34 | 2.67 |
| 5.0 | 98 | 98 | 2.26 | 1.88 |
| 10.0 | 75 | 81 | 1.32 | 1.10 |
| 25.0 | 57 | 49 | 0.56 | 0.44 |
| 50.0 | 37 | 37 | 0.32 | 0.26 |

[a] Estimated as $^1/_5$ of the recycle delay required for maximum signal intensity. [b] Measured via spin–echo delay.

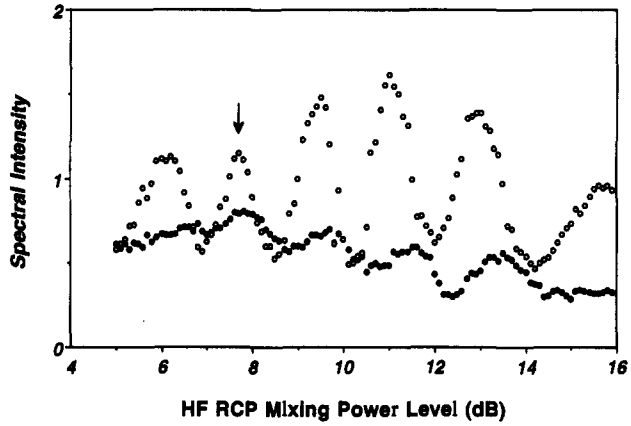


Figure 3. RCP signal intensities for 90% perdeuterated oxalic acid dihydrate as a function of proton mixing power at constant deuterium mixing power at room temperature. Open circles: total absolute spectral intensity. Filled circles: $COOH/2H_2O$ relative intensity. The arrow points to the condition used in the room-temperature 2D experiments, since the $COOH/2H_2O$ intensity ratio at this point matches that in Bloch decay spectra of the same sample.

$T_1$ increases faster than the dipolar coupling decreases as $r_{12}$ is increased by deuteration. This effect on the proton $T_1$ is illustrated in Table IV by room-temperature data for oxalic acid dihydrate. To obtain a fully relaxed one-dimensional spectrum with such long $T_1$'s, it is necessary to use a recycle delay which is prohibitively long for 2D spectroscopy.

Inspired by cross-polarization (CP) methods used widely in solid-state spectroscopy of rare spins,[13] we have developed a scheme for cross-polarizing protons from deuterons. Taking advantage of the relatively short deuterium $T_1$ (normally on the order of milliseconds due to the quadrupolar interaction), we can shorten the experimental recycle delay dramatically. Recently, Fyfe *et al.* reported using this same principle in cross-polarizing $^{31}P$ from $^{27}Al$ in their studies of the molecular sieve VPI-5.[14] Although the absolute signal intensity is much weaker with RCP than from a Bloch decay, the shorter recycle delay compensates and the overall signal-to-noise ratio per unit time is increased. Since the homonuclear dipolar coupling in the $^2H$ spin reservoir is weak (due to the small gyromagnetic ratio of $^2H$), the Hartmann–Hahn matching condition for this RCP scheme is narrow. Therefore, for each compound and each proton/deuteron ratio, the Hartmann–Hahn matching should be adjusted carefully. The spectral intensity measured as a function of $^1H$ field strength, with constant $^2H$ field strength and constant RCP mixing time, is illustrated in Figure 3 for 90% perdeuterated oxalic acid dihydrate and shows the oscillations expected when the abundant spin reservoir is weakly dipolar coupled.[15] The arrow in Figure 3 identifies the $^1H$ field strength used in our experiments. Here,

(13) Pines, A.; Gibby, M. G.; Waugh, J. S. *J. Chem. Phys.* **1973**, *59*, 569–590.

(14) Fyfe, C. A.; Grondey, H.; Mueller, K. T.; Wong-Moon, K. C.; Markus, T. *J. Am. Chem. Soc.* **1992**, *114*, 5876–5878.

(15) Stejskal, E. O.; Schaefer, J.; Waugh, J. S. *J. Magn. Reson.* **1977**, *28*, 105–112. Zeigler, R. T.; Wind, R. A.; Maciel, G. E. *J. Magn. Reson.* **1988**, *79*, 299–306. Meier, B. H. *Chem. Phys. Lett.* **1992**, *188*, 201–207.

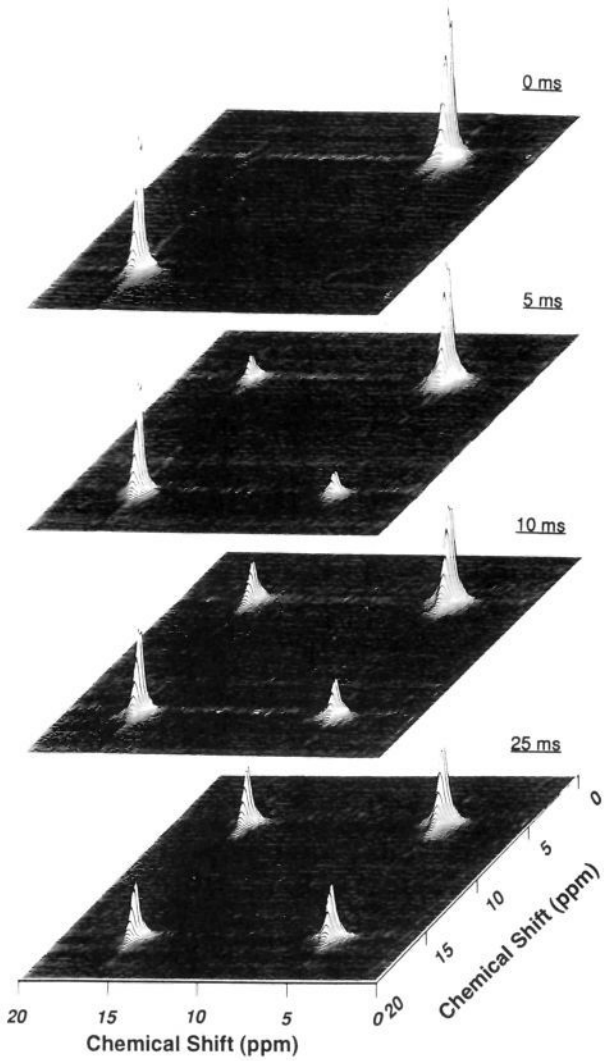


**Figure 4.** 2D $^1H$ spectra of 90% perdeuterated oxalic acid dihydrate with exchange mixing times varying from 0 to 25 ms.

the total spectral intensity (open circles) is at one of its maxima, and more importantly, the relative intensity of $COOH/H_2O$ matches that obtained from Bloch decay experiments.

**Two-Dimensional RCP Exchange Spectra.** Using RCP, $^1H$ spectra of deuterium spin-diluted solids can be acquired in a sufficiently short time to make two-dimensional $^1H$ studies feasible. Figures 4–7 show room-temperature 2D-RCP NOESY exchange spectra of perdeuterated oxalic acid dihydrate, aspartic acid, ammonium hydrogen oxalate hemihydrate (AHOX·$^1/_2H_2O$), and (AHOX:HOX)·$2H_2O$. The growth of the cross-peaks indicates the rate of proton exchange between the corresponding groups. The absence of cross-peak intensities in the spectrum of aspartic acid with a 200-ms mixing time (Figure 5) indicates the absence of proton exchange between the carboxyl and amino groups. Furthermore, Figure 5 shows that spin diffusion can be neglected in these magnetically dilute systems. In particular, significant cross-peak intensities due to spin diffusion are only observed after a 1600-ms mixing period. In contrast, AHOX·$^1/_2H_2O$ (Figure 6) shows rapid proton exchange between the amino group and the water of hydration, while cross-peaks involving the carboxyl group, developing only after 400 ms, may represent spin diffusion or very slow proton exchange.

## Discussion

**$^1H$ Chemical Shifts in Solids.** Table II lists $^1H$ chemical shifts for amino acids and model compounds relative to TMS. The

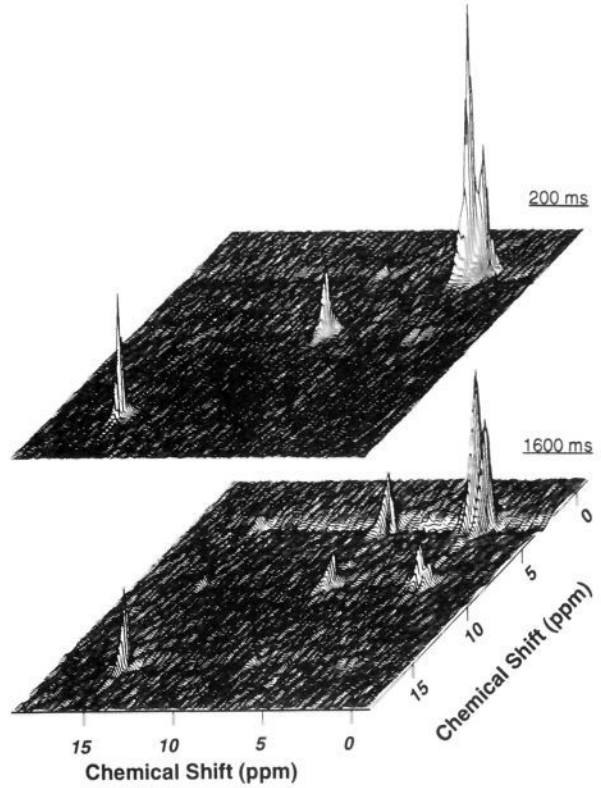


**Figure 5.** 2D $^1H$ spectra of perdeuterated aspartic acid with exchange mixing times of 200 and 1600 ms.

chemical shift values for the $CH_3$, $CH_2$, and CH protons agree well with published solution data.[9] However, the exchangeable protons are normally not observable by solution NMR. Even if these protons were detectable in solution, the chemical shifts might differ due to different hydrogen bonding in the solids and the solutions. The groups with exchangeable protons in our compounds are COOH, OH, $H_2O$, $NH_3^+$, and $NH_4^+$. Our $^1H$ chemical shift values for COOH groups vary from 12.5 to 16.6 ppm, which is consistent with the results of multiple pulse experiments,[9] and are further downfield than the commonly reported values of 10–12 ppm from solution measurement.[16] These differences suggest that the electronic environment of the COOH groups is very different in solids than in solutions. It is understood that the hydrogen bonding strength is very closely related to proton chemical shifts: the stronger the hydrogen bonding, the further downfield the shifts.[9] The same argument also can be applied to explain the chemical shift values of the water of hydration, which are found between 5.5 and 5.7 ppm, as compared to 4.8 ppm for bulk water. In general, our proton chemical shifts conform to the nonlinear correlation with O···H—O hydrogen bond strengths proposed by Kaliaperumal *et al.*[9]

**Isotope Effect.** While the ratio of water to carboxyl hydrogen protons in oxalic acid dihydrate is 2:1, our $^1H$ MAS Bloch decay spectra of several independent samples at and below room temperature reproducibly exhibited an intensity ratio of HOD:RCOOH less than 2:1. Water titration measurements on the deuterated oxalic acid dihydrate samples gave a mole ratio of 2:1, the stoichiometry expected from the crystal structure. We attribute the discrepancy in the observed spectral intensity ratio to an isotope effect, known as the "fractionation factor". To estimate this factor, the exchange reaction

$$\mathbf{R_0}: \quad \mathrm{RCOOD} + \mathrm{HOD} \overset{K_0}{\leftrightarrow} \mathrm{RCOOH} + \mathrm{DOD} \qquad (2)$$

(16) Dean, J. A. *Lange's Handbook of Chemistry*, 13th ed.; McGraw-Hill Book Co.: New York, 1985; p 8-43.

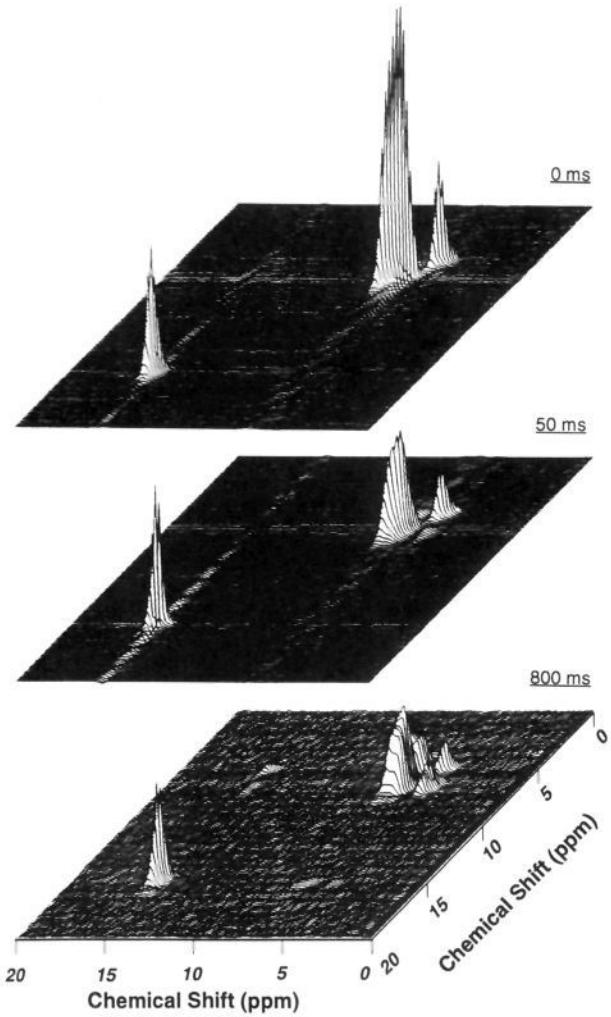


**Figure 6.** 2D $^1$H spectra of perdeuterated ammonium hydrogen oxalate hemihydrate (AHOX·$^1/_2H_2O$) with exchange mixing times of 0, 50, and 800 ms.

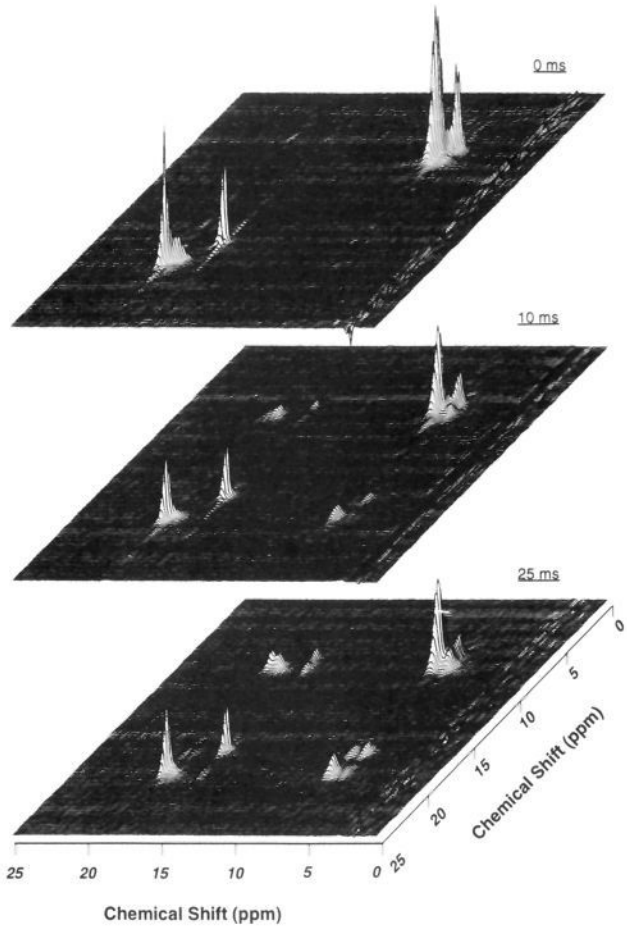


**Figure 7.** 2D $^1$H spectra of D-(AHOX:HOX)·$2H_2O$ with exchange mixing times of 0, 10, and 25 ms.

was decomposed into these four reactions:

$$\mathbf{R_1}: \quad \mathrm{RCOOD} \overset{K_1}{\leftrightarrow} \mathrm{RCOO^-} + \mathrm{D^+} \tag{3}$$

$$\mathbf{R_2}: \quad \mathrm{HOD} \overset{K_2}{\leftrightarrow} \mathrm{D^+} + \mathrm{OH^-} \tag{4}$$

$$\mathbf{R_3}: \quad \mathrm{RCOO^-} + \mathrm{H^+} \overset{K_3}{\leftrightarrow} \mathrm{RCOOH} \tag{5}$$

$$\mathbf{R_4}: \quad \mathrm{D^+} + \mathrm{OD^-} \overset{K_4}{\leftrightarrow} \mathrm{DOD} \tag{6}$$

The overall reaction has an equilibrium constant given by

$$K_0 = K_1K_2K_3K_4 \tag{7}$$

Using the relation[17]

$$\mathrm{pD} = \mathrm{pH(measured)} + 0.45 \tag{8}$$

to obtain $K_1$ and $K_2$, the ionization constant for $D_2O$ to obtain $K_4$, and the ionization constant for oxalic acid to obtain $K_3$, we estimated an intensity ratio of (1.76):1 at room temperature. The fractionation factor was also studied by Jarret and Saunders using solution $^{13}$C-NMR.[18] They reported HOD:RCOOH = (1.78):1 based on the change of $^{13}$C chemical shifts upon substitution of hydrogen isotopes at room temperature. Both the calculated estimate of 1.76:1 and the $^{13}$C-NMR result of 1.78:1 are for oxalic acid in solution. By comparison, our result of 1.64:1 for the most dilute case (proton atom 1%, spectrum not shown) suggests that the isotope effect is somewhat more pronounced in the solid state.

**Proton Exchange and Hydrogen-Bonded Chains.** The theory of the hydrogen-bonded chain (HBC) has been widely employed to explain proton conduction in a variety of solid systems,[19] including ice. Examining crystal structures of oxalic acid dihydrate,[20] aspartic acid,[21] AHOX·$^1/_2H_2O$,[6] and (AHOX:HOX)·$2H_2O$,[7] we found that hydrogen-bonded sites were associated with rapid proton exchange in the 2D NMR spectra. For example, in oxalic acid dihydrate hydrogen bonds connect the proton on each carboxyl group to a water molecule. Figure 4 shows that proton exchange between carboxyl and water sites in HOX·$2H_2O$ is observed within 5 ms. In AHOX·$^1/_2H_2O$, similar hydrogen bonding is observed between the ammonium groups and the water of hydration, while the carboxyl groups are only hydrogen bonded to each other. Therefore, the proton NMR 2D spectrum (Figure 6) shows that proton exchange is observed only between the ammonium and water groups. In the case of aspartic acid, the crystal structure shows no hydrogen bonds between –COOH and $-NH_3$ groups. This explains why we did not observe any exchange in Figure 5.

(17) Bates, R. G. In *Treatise on Analytic Chemistry*, 2nd ed.; Kolthoff, I. M., Elving, P. J., Eds.; John Wiley & Son: New York, 1978; Part I, Vol. 1, pp 821–863.

(18) Jarret, R. M.; Saunders, M. *J. Am. Chem. Soc.* **1985**, *107*, 2648–2654.

(19) Copeland, R. A.; Chan, S. I. *Annu. Rev. Phys. Chem.* **1989**, *40*, 671–698. Nagle, J. F.; Tristram-Nagle, S. *J. Membr. Biol.* **1983**, *74*, 1–14.

(20) Putkonen, M. L.; Feld, R.; Vettier, C.; Lehmann, M. S. *Acta Crystallogr.* **1985**, *B41*, 77–79.

(21) Derissen, J. L.; Endeman, H. J.; Peerdeman, A. F. *Acta Crystallogr.* **1968**, *B24*, 1349–1354.

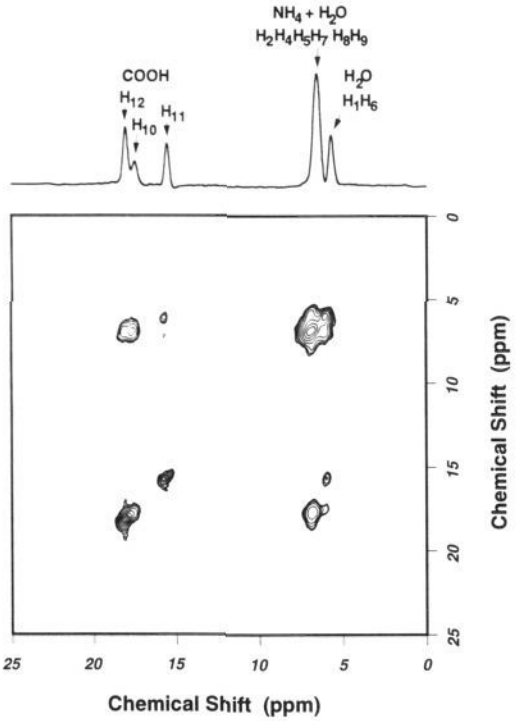


**Figure 8.** 1D proton spectrum and contour plot of the 2D spectrum with 10 ms exchange mixing time for (AHOX:HOX)·2$H_2O$.

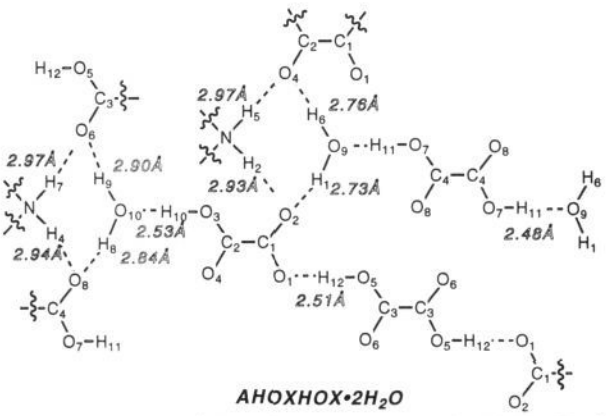


**Figure 9.** Illustration of the hydrogen bonds in (AHOX:HOX)·2$H_2O$.[7]

The most fascinating case is that of (AHOX:HOX)·2$H_2O$. As shown in Figures 7 and 8, there are three distinguishable carboxyl proton resonances (at 18.02, 17.54, and 15.52 ppm) and they exhibit distinct exchange behaviors. The carboxyl proton at 18.02 ppm does not show any rapid exchange with other protons, while the carboxyl protons at 17.54 and 15.52 ppm exchange rapidly, with different upfield protons. From this observation we conclude that the carboxyl protons in (AHOX:HOX)·2$H_2O$ form three different hydrogen bonds. This conclusion has been borne out by a follow-up X-ray diffraction study.[7] As illustrated in Figure 9, the crystal structure shows that one carboxyl proton ($H_{12}$) is involved in a hydrogen bond to the unprotonated oxygen of another carboxyl group. We assign this carboxyl proton to the 18.02-ppm signal. The other two carboxyl protons ($H_{10}$ and $H_{11}$) are hydrogen bonded to different water oxygens and are thus expected to exchange rapidly with the respective water protons. (Further exchange to other carboxyl groups is not expected because the water protons are hydrogen bonded only to unprotonated carboxyl oxygens). The hydrogen bonds of the water protons are appreciably shorter for one of the water molecules than for the other (O···O distances 2.73 and 2.76 Å vs 2.90 and 2.84 Å), so we assign the 5.71-ppm signal to the latter ($H_1$ and $H_6$) and the 6.54-ppm signal to the former ($H_8$ and $H_9$). The ammonia protons ($H_2$, $H_4$, $H_5$, and $H_7$) are also hydrogen bonded only to unprotonated carboxyl oxygens. These hydrogen bonds have an N···O distance of 2.92 to 2.97 Å and the corresponding hydrogen signal seems to overlap with the water proton signal at 6.54 ppm. These assignments are illustrated in the 1D spectrum in Figure 8.

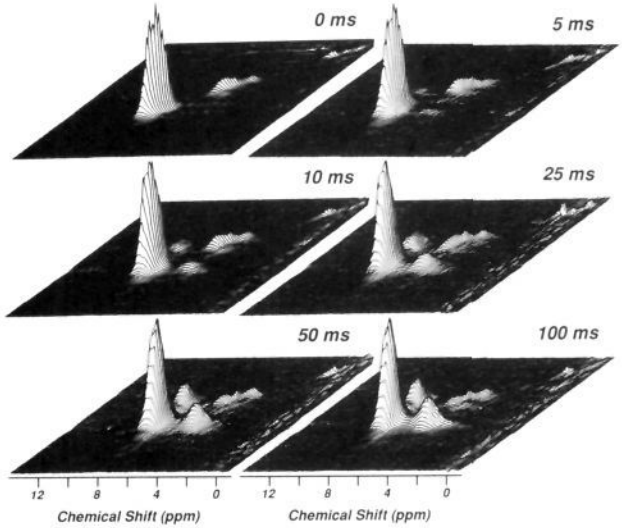


**Figure 10.** 2D $^1$H spectra of deuterated lithium hydrazinium sulfate with exchange mixing times varying from 0 to 100 ms. These spectra were taken with a recycle delay of 3 s without deuterium-to-proton cross-polarization.

The proton conductivity of HBCs has been best studied in inorganic crystals. For example, the crystal structure of lithium hydrazinium sulfate (LiHzS) shows that there is a HBC along the crystal polar axis,[22,23] while electrical measurements show nearly one-dimensional proton conductivity along this axis.[24] Figure 10 shows 2D proton exchange spectra of perdeuterated lithium hydrazinium sulfate. Since all the proton resonances in the spectra are due to protons in the hydrazinium ion ($N_2H_5^+$), definitive assignments for the various chemical shifts are difficult. However, we note from the crystal structure[22] that one of the protons in the $NH_2^+$ group is hydrogen bonded to another nitrogen, while the other four protons in the $N_2H_5^+$ ion are hydrogen bonded to oxygens of the sulfate ions. On the basis of the internuclear distances in the crystal structure, the N···O hydrogen bonds are stronger than the N···N hydrogen bond. Thus it is reasonable to assume, based on their relative intensities and chemical shifts, that the downfield peak belongs to the four protons in the N···O hydrogen bonds and the upfield peak belongs to the proton in the N···N hydrogen bond. On the basis of this assignment, we infer from the NMR cross-peaks that the hydrogen-bonded protons in this inorganic proton conductor exchange on a time scale similar to that seen in other hydrogen-bonded solids.

**Cross-Peak Intensities, Exchange Rate, and Activation Energy.** The use of two-dimensional NMR methods to study chemical exchange processes was pioneered by Jeener et al.[25] In 2D chemical exchange spectra, proton exchange between different sites during the mixing period gives rise to cross-peaks with intensities related to the corresponding exchange rates. The case for rapid (*i.e.* faster than proton relaxation) two-site exchange is described in the appendix. The development of cross-peak intensities with increasing exchange mixing time is plotted in

(22) Brown, I. D. *Acta Crystallogr.* **1964**, *17*, 654–663.
(23) Sebastian, M. T.; Becker, R. A.; Klapper, H. *J. Appl. Crystallogr.* **1991**, *24*, 1015–1022.
(24) Schmidt, V. H.; Drumheller, J. E.; Howell, F. L. *Phys. Rev. B* **1971**, *4*, 4582–4597.
(25) Jeener, J.; Meier, B. H.; Bachmann, P.; Ernst, R. R. *J. Chem. Phys.* **1979**, *71*, 4546–4553.

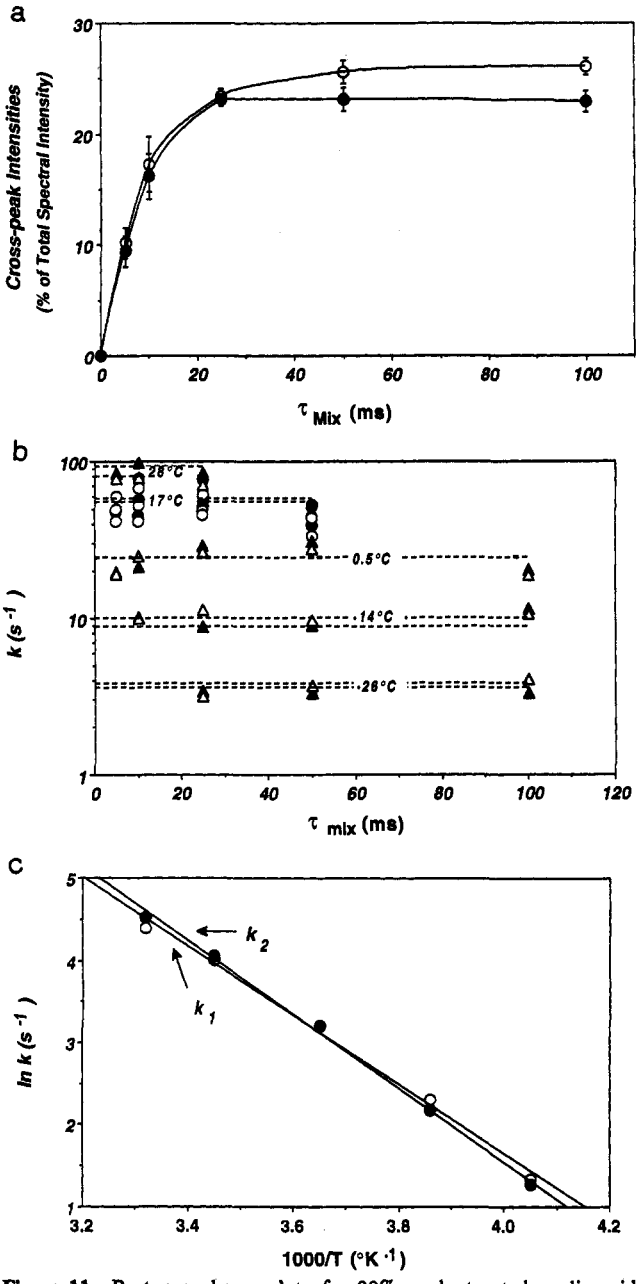


**Figure 11.** Proton exchange data for 90% perdeuterated oxalic acid dihydrate with exchange mixing times varying from 0 to 25 ms. Filled symbols represent data for $k_1$ in eq 9, and open symbols represent data for $k_2$. (a) Average intensity for each cross-peak in three experiments at room temperature. (b) The same room-temperature data (circles) and data for other temperatures (triangles), represented according to eqs A17 and A18. See text for details. (c) Relationship between proton exchange rates and temperature for oxalic acid dihydrate. Slopes yield Arrhenius activation energies for $k_1$ and $k_2$ in the temperature range 28 to -26 °C.

Figure 11a for proton exchange in oxalic acid dihydrate,

$$\text{R–COOD} + \text{HOD} \underset{k_2}{\overset{k_1}{\rightleftarrows}} \text{R–COOH} + \text{DOD} \qquad (9)$$

The two curves represent the average intensities for each of the two cross-peaks from three independent experiments. In Figure 11b, the data from these three sets of experiments are recast in the form of eqs A17–A19 of the Appendix. From these plots, we obtain the rates $k_1 = 55.2\ s^{-1}$ and $k_2 = 58.1\ s^{-1}$ for oxalic acid dihydrate at room temperature. Similar data for oxalic acid dihydrate at various temperatures from 28 to -26 °C are also presented in Figure 11b.

The temperature dependence of these exchange rates, obtained from Figure 11b, is plotted in Figure 11c. From this figure, we obtain Arrhenius activation energies of 8.4 kcal/mol for $k_1$ and 8.9 kcal/mol for $k_2$. These energy values fall into the upper range of the reported results from 2.9 to 11.8 kcal/mol obtained from both calculations and experiments[26] and are higher than those for *p*-toluic acid dimer measured by Meier *et al. via* single-crystal proton NMR.[27] These activation energies are well below the 19.1–20.3 kcal/mol energy levels for thermal dehydration of oxalic acid dihydrate.[28]

## Conclusion

When isotopic spin-dilution is chemically feasible, it offers an attractive alternative to multiple-pulse techniques for obtaining high-resolution $^1$H-SSNMR spectra in solids. The lengthening of the proton $T_1$ upon dilution can be overcome by reverse cross-polarization from deuterons to protons, yielding high-resolution proton 2D chemical exchange spectra in a reasonable amount of time. From such spectra, the rates and activation energies for proton exchange in solids can be determined. In model compounds we have found rapid proton exchange occurs along hydrogen bonds.

**Acknowledgment.** We thank A. E. McDermott for helpful discussions, J. M. Griffiths and J. R. Long for constructive critiques of the manuscript, and A. Thakkar and P. Allen for extensive technical assistance. This work was supported by grants from the National Institutes of Health (GM-36810, GM-23289, GM-23403, and RR-00995).

## Appendix

In a 2D NMR experiment, let $I_{XY}$ represent the population of spins at site X in the first time domain and at site Y in the second time domain.

For a two-site exchange:

$$\text{A} \underset{k_2}{\overset{k_1}{\rightleftarrows}} \text{B} \qquad (A1)$$

XY = AA or BB or AB or BA and the corresponding intensities are governed by the differential equations

$$dI_{AA}/dt = -k_1 \cdot I_{AA} + k_2 \cdot I_{AB} \qquad (A2)$$

$$dI_{BB}/dt = -k_2 \cdot I_{BB} + k_1 \cdot I_{BA} \qquad (A3)$$

$$dI_{AB}/dt = -k_2 \cdot I_{AB} + k_1 \cdot I_{AA} \qquad (A4)$$

$$dI_{BA}/dt = -k_1 \cdot I_{BA} + k_2 \cdot I_{BB} \qquad (A5)$$

The above differential eqs A2–A5 have solutions of the form

$$I_{XY}(t) = [I_{XY}(0) - I_{XY}(\infty)] \exp(-t/\tau) + I_{XY}(\infty) \qquad (A6)$$

By straightforward algebra it can be shown that $\tau = (k_1 + k_2)^{-1}$ and, since $I_{AB}(0), I_{BA}(0) = 0$,

$$I_{AA}(t)/I_{AA}(0) = \exp(-t/\tau) + k_2\tau[1 - \exp(-t/\tau)] \qquad (A7)$$

$$I_{BB}(t)/I_{BB}(0) = \exp(-t/\tau) + k_1\tau[1 - \exp(-t/\tau)] \qquad (A8)$$

$$I_{AB}(t)/I_{AA}(0) = k_1\tau[1 - \exp(-t/\tau)] \qquad (A9)$$

$$I_{BA}(t)/I_{BB}(0) = k_2\tau[1 - \exp(-t/\tau)] \qquad (A10)$$

(26) Scheiner, S. *Acc. Chem. Res.* **1985**, *18*, 174–180. Jeffrey, G. A.; Saenger, W. *Hydrogen Bonding in Biological Structures*; Springer-Verlog: Berlin, 1991; Chapter 2.
(27) Meier, B. H.; Graf, F.; Ernst, R. R. *J. Chem. Phys.* **1982**, *15*, 767–774.
(28) Tanaka, H. *J. Thermal. Anal.* **1984**, *29*, 1115–1122. Tanaka, H.; Kawabata, K. *Thermochim. Acta* **1985**, *92*, 219–222.

Notice that, as expected,

$$I_{AA}(t) + I_{AB}(t) = I_{AA}(0) \tag{A11}$$

$$I_{BB}(t) + I_{BA}(t) = I_{BB}(0) \tag{A12}$$

If we define

$$R_A(t) = I_{AB}(t)/I_{AA}(0) = \{1 + [I_{AA}(t)/I_{AB}(t)]\}^{-1} \tag{A13}$$

and

$$R_B(t) = I_{BA}(t)/I_{BB}(0) = \{1 + [I_{BB}(t)/I_{BA}(t)]\}^{-1} \tag{A14}$$

then the sum of eqs A9 and A10 can be written as

$$[1 - \exp(-t/\tau)] = R_A(t) + R_B(t) \tag{A15}$$

So that

$$\tau = -t/\ln\{1 - [R_A(t) + R_B(t)]\} \tag{A16}$$

Substituting into eqs A9 and A10 separately, it follows that

$$k_1 = R_A(t)/Q(t) \tag{A17}$$

and

$$k_2 = R_B(t)/Q(t) \tag{A18}$$

where

$$Q(t) = -[R_A(t) + R_B(t)] \ln\{1 - [R_A(t) + R_B(t)]\}/t \tag{A19}$$